Urea derivatives carrying a thiophenylthiazole moiety: Design, synthesis, and evaluation of antitubercular and InhA inhibitory activities

Rüveyde Keleş Atıcı, Şengül Dilem Doğan, Miyase Gözde Gündüz, Vagolu Siva Krishna, Melina Chebaiki, Håvard Homberset, Christian Lherbet, Tone Tønjum, Lionel Mourey

Urea derivatives carrying thiophenylthiazole moiety: Synthesis and evaluation of antitubercular and InhA inhibitory activities

Rüveyde Keleş[a], Şengül Dilem Doğan[a*], Miyase Gözde Gündüz[b], Vagolu Siva Krishna[c], Melina Chebaiki[d,e], Håvard Homberset[c], Christian Lherbet[e], Tone Tønjum[c,f], Lionel Mourey[d]

[a]Department of Basic Sciences, Faculty of Pharmacy, Erciyes University, 38039, Kayseri, Turkey

[b]Department of Pharmaceutical Chemistry, Faculty of Pharmacy, Hacettepe University, Sıhhiye, 06100, Ankara, Turkey

[c]Unit for Genome Dynamics, Department of Microbiology, University of Oslo, Oslo, Norway

[d]Institut de Pharmacologie et de Biologie Structurale, IPBS, Université de Toulouse, CNRS, UPS, 31077 Toulouse, France.

[e]LSPCMIB, UMR-CNRS 5068, Université Paul Sabatier-Toulouse III, 118 Route de Narbonne, 31062 Toulouse Cedex 9, France

[f]Division of Laboratory Medicine, Department of Microbiology, Oslo University Hospital, Oslo, Norway

*Corresponding author

Dr. Şengül Dilem Doğan

Address: Erciyes University
Faculty of Pharmacy
Department of Basic Sciences
38039
Kayseri, TURKEY

E-mail address: dogandilem@gmail.com
Phone number: +90 352 2076666-28032

Abstract

The greatest impediment to bringing the infections caused by *Mycobacterium tuberculosis* under control is the rising of strains that developed resistance to clinically used molecules. Therefore, the discovery of novel drug candidates for the treatment of this challenging disease is becoming dramatically more important. Prompted by this situation, we rationally designed and synthesized sixteen compounds carrying thiophene and thiazole rings beside the core urea functionality (**TTU1-TTU16**) through the combination of antitubercular pharmacophores. Following their extensive structural characterization, the obtained compounds were initially evaluated for their antimycobacterial activity against *Mycobacterium tuberculosis* H37Rv. Subsequently, three derivatives standing forward with their outstanding biological profiles and low cytotoxicities were tested on the drug (isoniazid)-resistant clinical isolates carrying *katG* and *inhA* mutations. Additionally, due to their pharmacophore similarities to the well-known InhA inhibitors, all molecules were screened for their enoyl acyl carrier protein reductase (InhA) inhibitory potentials. Molecular docking studies were finally performed to support the experimental enzyme inhibition data.

Keywords: thiophene, thiazole, enoyl acyl carrier protein reductase, antimycobacterial, molecular docking, drug-resistant clinical isolates

1. Introduction

Tuberculosis (TB), primarily caused by *Mycobacterium tuberculosis* (*Mtb*), is a contagious bacterial infection and still poses a severe global threat to human health despite existing since ancient times [1]. World Health Organization (WHO) designated TB to be the main cause of death attributable to a single infectious agent, with an estimated ten million individuals contracting the disease in 2020 [2].

Despite the recently marketed molecules such as bedaquiline and delamanid in addition to the current antitubercular drugs, TB therapy remains a severe challenge worldwide [3]. The greatest roadblock to the success of the existing TB chemotherapeutic regime is the emergence of drug-resistant strains [4]. This situation highlights the urgent need for the discovery of novel antimycobacterial compounds with different scaffolds.

Thiazole is a five-membered heterocyclic ring carrying both sulfur and nitrogen atoms holding an important position among all heterocycles due to its established significance in medicinal chemistry [5]. This prominent scaffold often acts as a strategic pharmacophore in therapeutically valuable molecules with versatile biological applications including anticancer, antidepressant and anti-inflammatory [6–8]. Thiazole is present in the structures of many commercial anti-infective agents such as sulfathiazole and acinitrazole (antibacterial), thiabendazole (antiparasitic), and abafungin (antifungal) (Figure 1) [9]. Additionally, this valuable scaffold plays an important role in the design and discovery of new antitubercular compounds [10]. Therefore, it is obvious that thiazole ring possesses a definite capacity to disrupt the critical metabolic processes of the infectious agents.

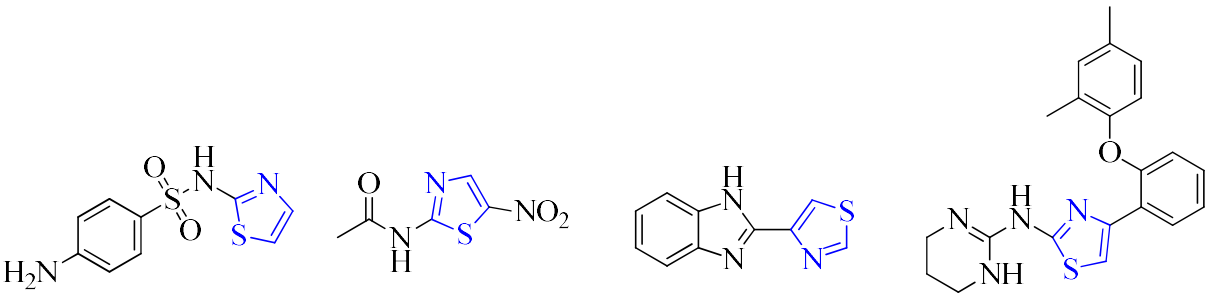

Figure 1. Chemical structures of commercial anti-infective agents carrying thiazole rings.

Thiophene is another sulfur-containing ring and represents one of the most frequent heterocycles in biologically active compounds including antitubercular agents [11–13].

The urea functionality has a central role in the drug design process due to its ability to establish hydrogen bonds regarded as one of the most important drug-biological target interactions [14].

This pharmacophore also serves as a key building block in the synthesis of biologically active molecules ranging from antitubercular to anticancer agents, as well as numerous clinically authorized drugs (Figure 2) [15,16].

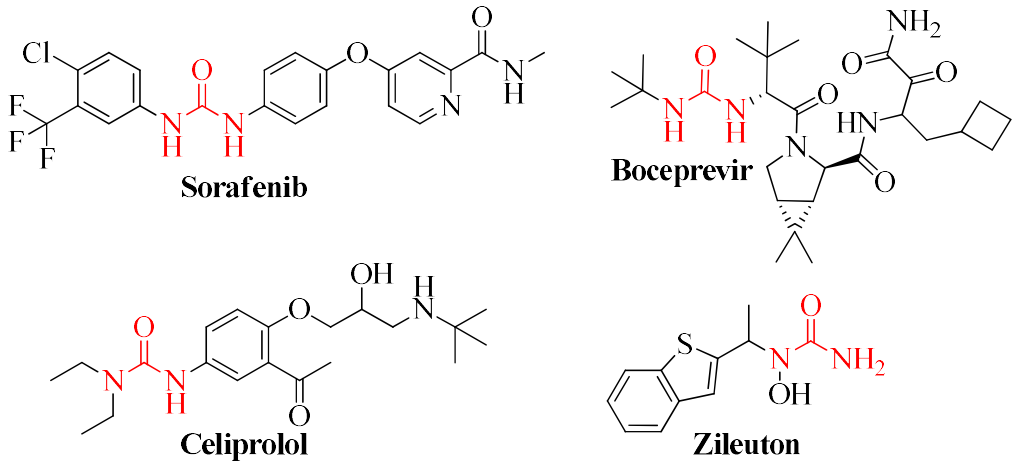

Figure 2. Representative examples of urea-containing FDA-approved drug molecules.

Enoyl acyl carrier protein reductase, InhA, is one of the critical enzymes employed in the fatty acid biosynthesis pathway of *Mtb* [17]. As fatty acids, mainly mycolic acids, are essential components of the bacterial cell wall, they are of utmost importance for the survival of *Mtb* [18]. Therefore, InhA stands as an attractive target for the development of new antitubercular agents. This NADH-dependent enzyme is also the principal target of isoniazid (isonicotinic acid hydrazide, INH) which is one of the first-line antitubercular drugs [19]. Being a prodrug, INH has to be activated by KatG, a catalase-peroxidase enzyme, to block InhA. Following this activation, isoniazid forms unstable species that readily react with the cofactor NADH to generate a covalently bound adduct [20,21]. Consequently, the mutations in *katG* diminish this activation yielding the most common type of drug resistance to INH [22]. Therefore, it is critical to design and develop novel compounds that directly target the binding pocket of InhA instead of requiring KatG activation for the efficient treatment of TB.

Although the binding site of InhA can be occupied by various chemically diversified molecules (Figure 3), in almost all circumstances, the direct inhibitors of InhA interact with the enzyme via hydrogen bonds to the cofactor (NADH) and a tyrosine residue (Tyr158) in addition to the hydrophobic contacts with the lipophilic pockets [23].

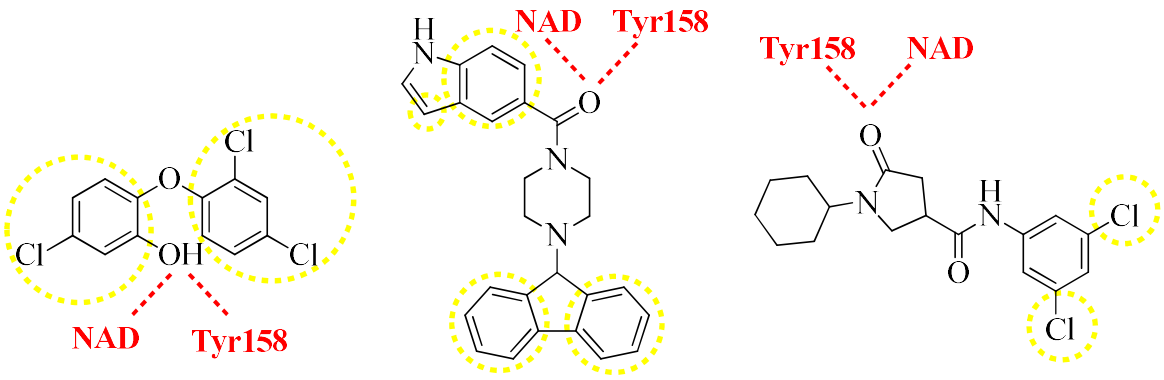

Figure 3. Chemical structures of representative InhA inhibitors co-crystallized in the enzyme deposited in Protein Data Bank (PDB) with the mentioned codes. Molecular parts providing InhA binding are highlighted: hydrophobic contacts and hydrogen bonds are shown as yellow spheres and red dotted lines, respectively.

Prompted by the mentioned considerations, we aimed to combine thiophene and thiazole rings, as well as urea functionality (**TTU1-TTU16**) in the same molecules (Figure 4). We extensively screened the obtained compounds for their antitubercular activities. As our compounds possess the required pharmacophores for targeting InhA, hydrogen bond participating atoms/groups for NAD and Tyr158 binding in addition to terminal hydrophobic rings, we also evaluated the InhA inhibition capacities of the synthesized molecules.

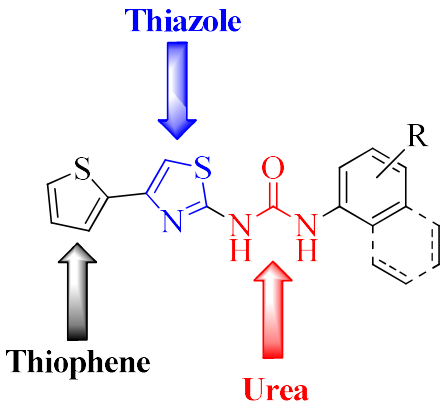

Figure 4. The design approach and general chemical structures of the target molecules.

.

2. Results and discussion

2.1. Chemistry

The synthetic pathways for preparing the final compounds are summarized in Scheme 1. The starting scaffold 4-(thiophen-2-yl)thiazol-2-amine (**IV**) was obtained according to reported protocols. Briefly, it was prepared by bromination of 2-acetylthiophene (**I**) with bromine in methylene chloride to give α-bromoketones (**II**). Subsequent cyclization reaction of α-bromoketones (**II**) with thiourea (**III**) under mild basic conditions afforded the corresponding 4-(thiophen-2-yl)thiazol-2-amine (**IV).** The obtained 4-(thiophen-2-yl)thiazol-2-amine (**IV)** was then used for the synthesis of the targeted urea derivatives **TTU1-TTU16.** The first synthetic approach for the synthesis of urea derivatives involved the stirring of 4-(thiophen-2-yl)thiazol-2-amine (**IV)** with commercially available isocyanates in dry benzene overnight at reflux conditions resulting in the formation of the respective urea derivatives **TTU3**, **TTU5-TTU7**, **TTU9-TTU11**, **TTU13**, and **TTU16**. Alternatively, the remaining urea derivatives were achieved from corresponding acyl azides **VII** which were obtained by the treatment of benzoic acid derivatives (**VI**) with ethyl chloroformate in the presence of triethylamine followed by the addition of NaN_3 aqueous solution. Refluxing the acyl azide in dry aprotic solvent (benzene) initiated rearrangement (Curtius rearrangement) to the corresponding isocyanate which was then reacted with amine **IV** to produce the corresponding urea derivatives **TTU1, TTU2**, **TTU4**, **TTU8**, **TTU12**, **TTU14**, and **TTU15**.

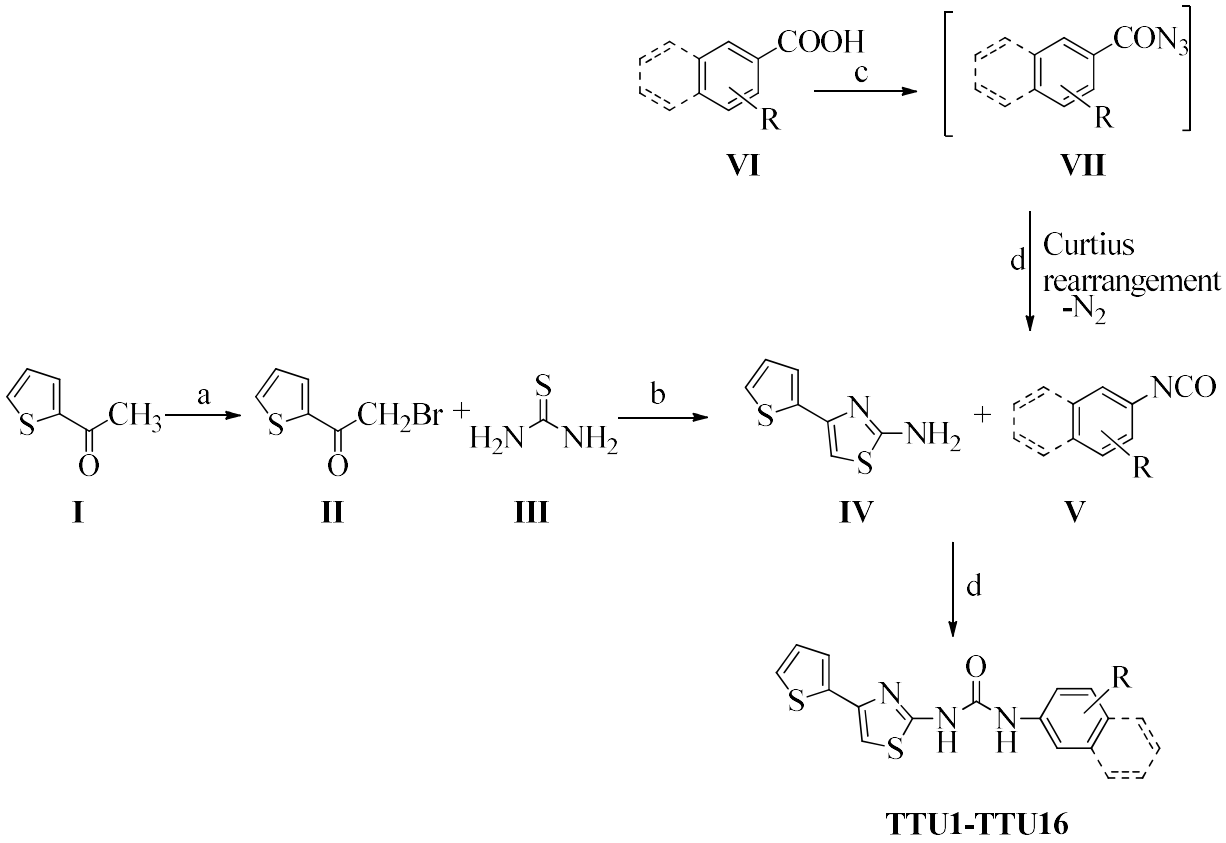

Scheme 1. Reagents and conditions: (**a**) Bromine, DCM, 0 °C to rt, 2 h. (**b**) Ethanol, reflux, 2 h. (**c**) i. Et_3N, ethyl chloroformate, THF ii. NaN_3/H_2O. (**d**) Benzene, reflux.

The structures of the urea derivatives were confirmed by ^{1}H-NMR, ^{13}C-NMR, HRMS. The presence of two exchangeable singlet signals at δ 11.20 – 10.72 and 9.50 – 8.63 ppm, corresponding to protons of NH*a* and NH*b* of the urea moiety, was observed in the NMR spectra of compounds **TTU1-TTU16**. The ^{13}C NMR spectra of these compounds displayed signals at δ160.95 - 159.10 ppm attributed to the carbon of urea carbonyl. ^{1}H-NMR and ^{13}C-NMR spectra of **TTU1-TTU16** are provided as supplementary materials.

2.2. Antitubercular activity determination and cytotoxicity evaluation

We tested all synthesized molecules (**TTU1-TTU16**) for their antitubercular activities against *Mtb* H37Rv and some of these against two INH-resistant (InhA mutant and KatG mutant) clinical isolates by applying Microplate Alamar Blue Assay (MABA) method. The initial screening results of the compounds at 1.56 - 200 µM concentration against *Mtb* H37Rv are represented as minimum inhibitory concentration (MIC) along with cytotoxicity of the most active derivatives in Table 1.

Table 1. Chemical structures, MIC values against *Mycobacterium tuberculosis* H37Rv and cytotoxicity data of the synthesized compounds

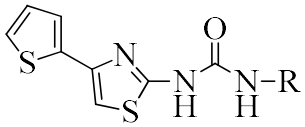

			Toxicity Data	
Compound	**R**	**MIC (µM)**	**IC_{50}(µM)[a]**	**%Inhibition[b]**
TTU1	4-bromophenyl	>200		
TTU 2	4-chlorophenyl	>200		
TTU 3	3-fluorophenyl	25		
TTU 4	4-fluorophenyl	50		
TTU 5	3-cyanophenyl	<1.56	14.21	22.55
TTU 6	4-cyanophenyl	3.125	7.26	24.31
TTU 7	4-(trifluoromethyl)phenyl	200		
TTU 8	4-nitrophenyl	>200		
TTU 9	*m*-tolyl	12.5		
TTU10	*p*-tolyl	>200		
TTU11	4-(*tert*-butyl)phenyl	12.5		
TTU12	4-methoxyphenyl	1.56	8.15	28.85
TTU13	4-chloro-3-(trifluoromethyl)phenyl	100		
TTU14	3,4-dimethoxyphenyl	12.5		
TTU15	3,4,5-trimethoxyphenyl	>200		
TTU16	2-naphthyl	50		
INH		<1.56		

[a] IC50: Concentration required to inhibit cell growth of HEK cells by 50%
[b] Inhibition is determined for 25 µM concentration of test compound

Except for **TTU16** with naphthyl group, the compounds differ from each other through the substitution pattern of their phenyl rings. Consequently, the type and position of the phenyl substituents directly determine the activity profile of the synthesized compounds. Based on the obtained MIC values, **TTU5** carrying cyano group at meta position of the phenyl ring was found to be the most active antitubercular member of this series. It is noteworthy that changing the position of this cyano group from C-3 to C-4 of the phenyl moiety yielded another active compound; **TTU6** with MIC value of 3.125 µM. **TTU12** was also an attractive compound, with an antimycobacterial MIC value of 1.56 µM, possessing methoxy group at the para position of the phenyl ring. While introducing the second methoxy substituent into the mentioned ring decreased the antitubercular efficacy (**TTU14-**12.5 µM), the third methoxyl group in the structure of **TTU15** destroyed the activity. **TTU9** and **TTU11** were moderate inhibitors of *Mtb*, with MIC values of 12.5 µM, carrying methyl and *tert*-butyl groups, respectively as alkyl substituents on the phenyl ring. Although adding alkyl groups were among the favorable modifications, condensing another phenyl ring yielding the naphthyl group (**TTU16**) diminished the biological activity.

Toxicity to the healthy cells appears as a severe problem while developing new antimycobacterial agents. Therefore, we screened the three most active derivatives from the initial test (**TTU5**, **TTU6**, and **TTU12**) for their cytotoxicity against HEK cells using MTT assay. According to the obtained data, these bioactive compounds were also found to be nontoxic with < 50% inhibition value.

Afterwards, we screened **TTU5**, **TTU6**, and **TTU12** along with isoniazid again to determine their MIC_{50} values (Figure 5).

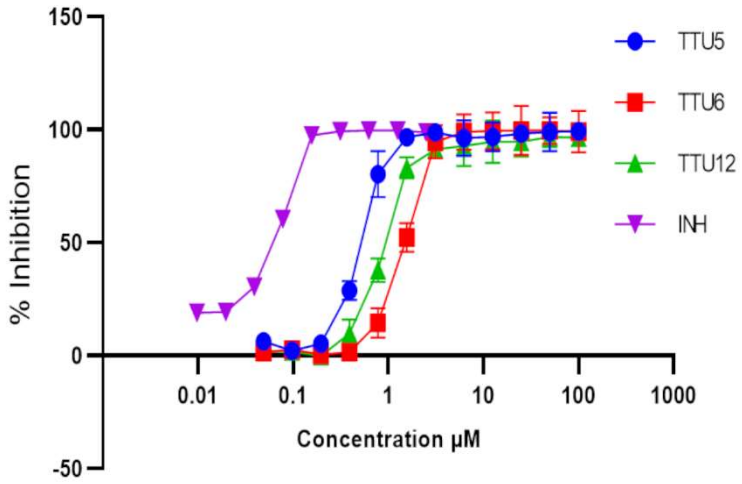

Compound	IC_{50} ± SD
TTU5	0.51±0.3 µM
TTU6	1.43±0.5 µM
TTU12	0.88±0.1 µM
INH	0.07±0.02 µM

Figure 5. MIC_{50} ± SD values calculated for the selected compounds and INH with GraphPad Prism. n = 3.

The resistance developed by *Mtb* against INH is linked to the presence of mutations in the *katG* and *inhA* genes [24]. Therefore, we also evaluated antitubercular activities of the selected compounds (**TTU5**, **TTU6**, and **TTU12**) as well as INH against INH-resistant *Mtb* clinical isolates mutated in *katG* and *inhA*. With this aim, we treated such isolates carrying *inhA* and *katG* mutations with increasing concentrations of the compounds and monitored them in the MABA assay. The obtained data and MIC_{50} values of the mentioned compounds are provided in Figure 6.

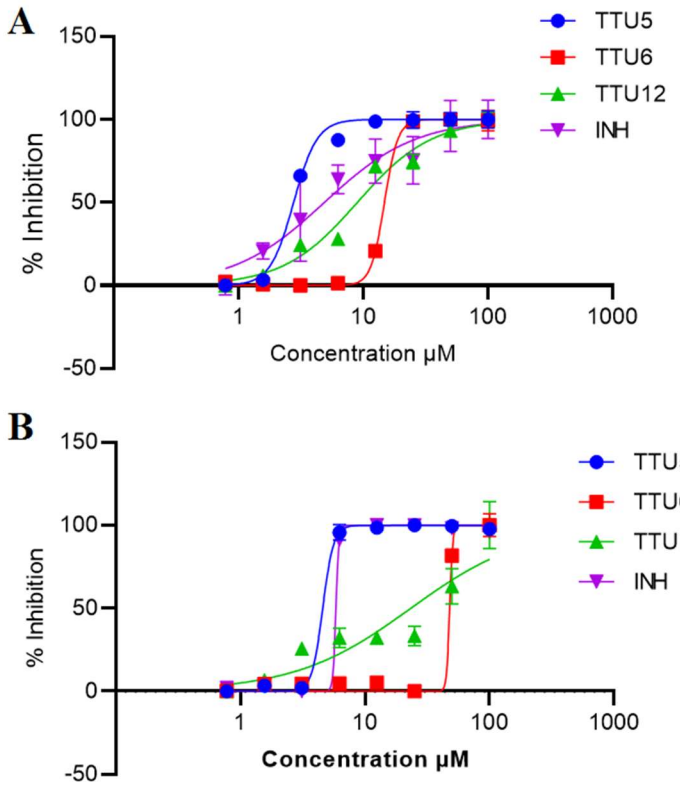

Compound	IC_{50} ± SD
TTU5	2.75±0.3 µM
TTU6	14.76±1.3 µM
TTU12	8.93±2.5 µM
INH	4.86±1.5 µM

Compound	IC_{50} ± SD
TTU5	4.59±0.6 µM
TTU6	47.92±1.6 µM
TTU12	23.34±1.3 µM
INH	6.25±2.4 µM

Figure 6. MIC_{50} ± SD values calculated with GraphPad Prism for **TTU5**, **TTU6**, **TTU12**, and INH against INH-resistant *Mtb* clinical isolates carrying *inhA* (A) and *katG* (B) mutations, n=3.

Based on the obtained values, it is obvious that MIC_{50} values of INH against drug-resistant clinical isolates are considerably higher than the one calculated for *Mtb* H37Rv. Additionally, **TTU5** showing the lowest MIC value against *Mtb* H37Rv was also the most effective derivative on both *inhA* and *katG* mutant INH-resistant strains even with better MIC_{50} values than those of isoniazid.

2.3. InhA inhibition assay

The discovery of direct inhibitors of InhA is of utmost importance due to drug-resistant *Mtb* strains. The binding pocket of the enzyme can tolerate inhibitors with highly different chemical

structures and volumes as long as the main structural requirements are met. As can be seen in Figure 7, the common pharmacophores of triclosan (TCL) and GEQ, well-known InhA inhibitors, are hydrogen-bond forming groups located in the center of the compounds and terminal rings for hydrophobic contacts.

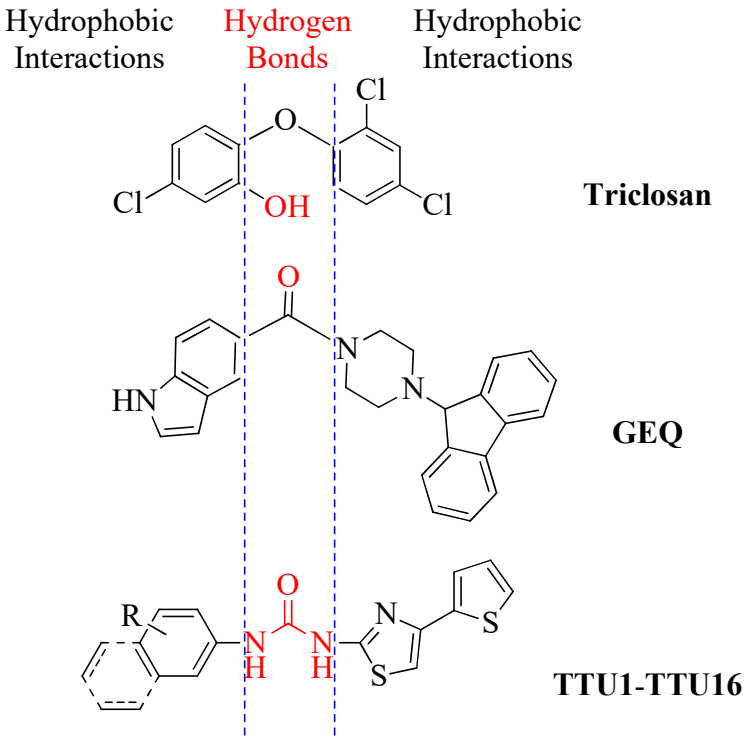

Figure 7. Representation of pharmacophore similarities between title molecules and well-known InhA inhibitors

As our compounds also provide these strategic pharmacophores to interact with InhA, we screened **TTU1-TTU16** for their *in vitro* inhibition capacities of InhA from *Mtb* at 50 µM employing triclosan as a positive control (Table 2).

Table 2. InhA inhibition values for **TTU1-TTU16** and **TCL** at 50 µM concentration.

Compound	% Inhibition
TTU1	62 (4 at 10 µM)
TTU2	43
TTU3	28
TTU4	27
TTU5	16
TTU6	17
TTU7	22
TTU8	19

TTU9	24
TTU10	26
TTU11	22
TTU12	25
TTU13	8
TTU14	4
TTU15	10
TTU16	19
TCL	98

TCL: Triclosan. All assays were carried out in triplicate.

According to the obtained inhibition values, two compounds stand forward in the tested compounds. **TTU2** was a modest inhibitor of InhA activity with 43% inhibition. The best inhibitor among this series was **TTU1** showing 62% inhibition value against InhA at 50 μM. When the results were analyzed in terms of the chemical structures of the compounds, it can be seen that **TTU1** and **TTU2** carry bromine and chlorine atoms, respectively at the *para* position of their phenyl rings. As the main structural difference of the compounds is the substitution pattern of the phenyl ring, we can conclude that lipophilic halogens at the *para* position of this ring are preferential for InhA inhibitor activity. The lack of inhibition against InhA, for **TTU5** and **TTU12** in contrast with their low MICs suggests that their targets are not mainly InhA. These new derivatives present a mode of action different of Triclosan and other relative compounds making them interesting candidates for further drug design in *Mtb* drug research.

2.4. Molecular docking

To rationalize InhA inhibition by **TTU1,** we used *in silico* docking of this compound into the active pocket of the InhA enzyme. The proposed binding mode of **TTU1** and the interaction patterns are represented in Figure 8.

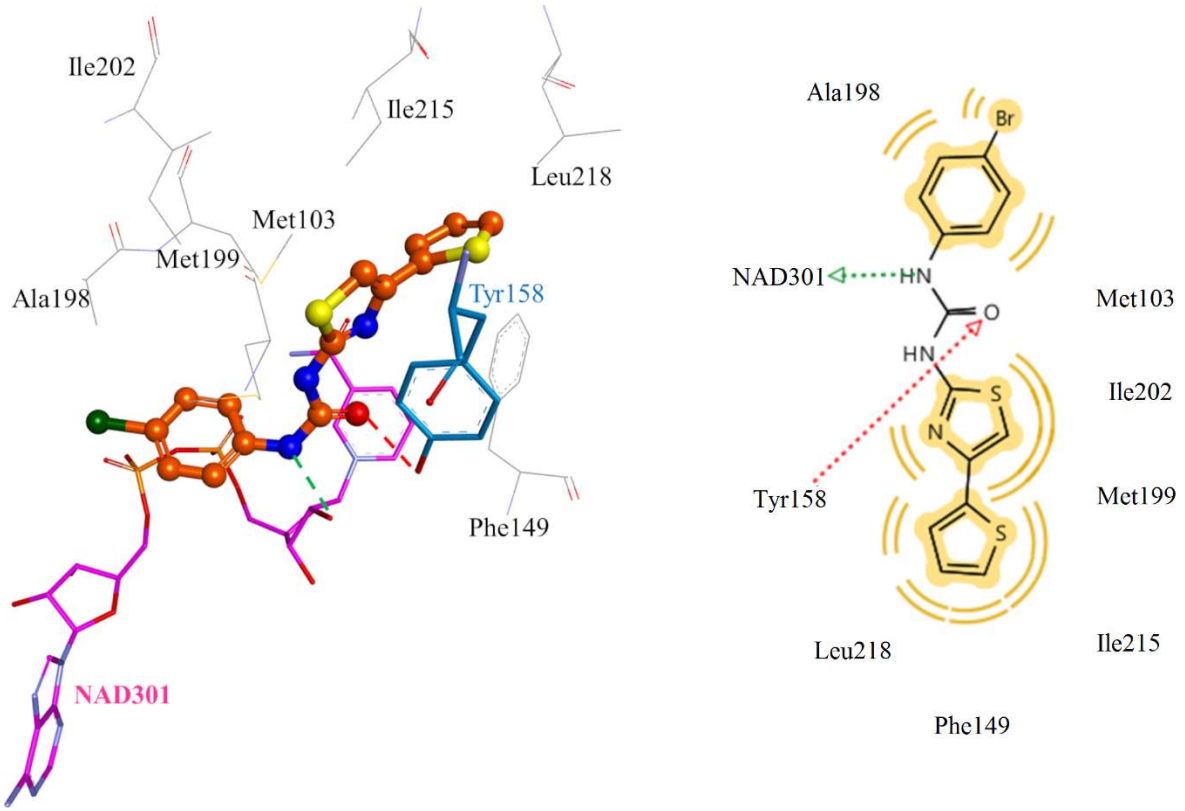

Figure 8. Suggested docking pose of **TTU1** in the binding site of InhA (A) and 2D interaction map (B). **TTU1** is shown as orange balls and sticks. Amino acid residues contributing to hydrophobic interactions are represented as black lines. The NAD cofactor and residue Tyr158 are highlighted as pink and cyan sticks, respectively. Interaction types: red arrow, hydrogen bond acceptor; green arrow, hydrogen bond donor; yellow spheres, hydrophobic contacts.

Docking of **TTU1** indicates that the urea functionality plays a key role in the interactions with the InhA enzyme. The urea carbonyl forms a hydrogen bond with Tyr158 and one of the NH groups interacted with the ribose group of the cofactor (NAD301) through an additional hydrogen bond. Furthermore, both thiazole and thiophene rings are engaged in hydrophobic contacts with multiple amino acid residues constituting the lipophilic pocket of the binding site. In addition to the lipophilic contact of the phenyl moiety, it is noteworthy that the bromine atom borne wy the phenyl ring forms hydrophobic interaction with Ala198.

3. Conclusions

TB continues to critically jeopardize human health worldwide due to the emergence of drug-resistant strains of *Mtb* appearing as a formidable challenge. Thus, this situation highlights the urgent need for the discovery of molecules with novel scaffolds. We presented herein the design and the synthesis of urea-based derivatives carrying thiazole and thiophene rings, which frequently take place in the structures of antimycobacterial agents. Following biological tests on *Mtb* H37Rv and INH-resistant strains, we identified active molecules also capable of acting

against drug-resistant clinical isolates. Cyano and methoxy substituents on phenyl ring were preferential for the antitubercular activity. Prompted by their common pharmacophores defined for InhA inhibitors, the compounds were additionally screened for their InhA inhibition capacities. Based on the obtained values, lipophilic halogens on the phenyl ring led to an increase in the inhibition potential. Altogether, our study may provide future perspectives in the design and development of new antitubercular agents for the improvement of the current treatment regimens.

4. Material and methods

4.1. Chemistry

4.1.1. Experimental

Just before use, THF and benzene were distilled from sodium-benzophenone. All reagents were used as received. All volatiles were removed under reduced pressure. Reaction progress was monitored by TLC using silica gel 60 F254 (0.040–0.063 mm) with detection by UV. Infrared (IR) spectra were obtained via ATR diamond in the range 4000–600 cm^{-1}. ^{1}H NMR (400 MHz) spectra and ^{13}C NMR (100 MHz) spectra were recorded on a Bruker AM 400 MHz NMR spectrometer with DMSO-*d*6 as the solvent. The multiplicities of NMR signals are designated as s (singlet), d (doublet), dd (double doublet), t (triplet), q (quartet), br (broad), m (multiplet, for unresolved lines). The values of chemical shifts (δ) are given in ppm and coupling constants (*J*) in Hertz (Hz). The yields are referred to purified products and are not optimized. Open glass capillaries were used to determine melting points, which were not uncorrected.

4.1.2. Synthetic procedures

Synthesis of 2-(bromoacetyl)thiophene (II)

2-(Bromoacetyl)thiophene (**II**) was synthesized according to the modified literature procedure [25]. 2-Acetylthiophene was added dropwise to a bromine in dichloromethane solution that had been chilled to 0 °C and stirred for 5 minutes at 0 °C. The reaction was then allowed to cool to 25°C before being stirred for 2 hours. After that, a saturated sodium hydrogen carbonate was added to neutralize the mixture, and dichloromethane was used to extract the mixture (3x25 mL). The combined organic layers were washed with brine, dried over $MgSO_4$ and concentrated in vacuo. For the next stage, a pale yellow oil product was used without being purified.

Synthesis of 4-(thiophen-2-yl)thiazol-2-amine (IV)

These compounds were synthesized according to the modified literature procedure [26,27]. 2-Bromoacetylthiophene (**II**) (1 equiv.) and thiourea (**III**) (1.25 equiv.) in ethanol (20 mL) were stirred for 15 min at 25 °C. After this, the reaction was stirred at 80 °C for 2 h. The reaction mixture was made alkaline after cooling using a 10% sodium hydroxide solution, obtaining a precipitate that was filtered to give **IV** as white solid. The desired chemical was obtained after recrystallization with ethanol. Mp 124-126°C; ^{1}H NMR (400 MHz, DMSO-d_6) δ 7.37 (dd, J = 8.0, 4.2 Hz, 2H), 7.17 (s, 2H), 7.09 – 6.97 (m, 1H), 6.83 (s, 1H).^{13}C NMR (100 MHz, DMSO) δ 168.72, 144.90, 139.62, 128.19, 125.14, 123.19, 100.22. HRMS (EI): $[M+H]^+$, found 183.00452. $C_7H_6N_2S_2$ requires 183.00694).

General procedure for the synthesis of 1-phenyl-3-(4-(thiophen-2-yl)thiazol-2-yl)urea derivatives (TTU1, TTU2, TTU4, TTU8, TTU12, TTU14, TTU15)

Triethylamine (1 equiv.) in 5 mL THF was added dropwise to a solution of corresponding benzoic acid (VI) (1 equiv.) in 10 mL THF at -5 °C. After 30 minutes, add the cooled ethyl chloroformate solution (1 equiv.) in 5 mL THF gently and stir for 30 minutes at -5 °C. In the final stage, a drop-by-drop solution of sodium azide (2 equiv.) in 5 mL water was added and stirred overnight at room temperature. Ethyl acetate (3x15 mL) was used to extract the resultant mixture and the organic phase was washed with saturated sodium bicarbonate (3 × 30 mL) and with water (2 × 25 mL) and dried over $MgSO_4$. The corresponding azide was obtained after the ethyl acetate was removed. The acquired acyl azide was used instantly without any purification [28,29]. Obtained acyl azide (**VII**) (1 equiv.) and 4-(thiophen-2-yl)thiazol-2-amine (**IV)** (1 equiv.) in benzene (20 mL) was stirred at 70–80 °C for 24 h. The precipitate that had formed was filtered out and washed with benzene. The urea derivatives were obtained after the residue was purified by crystallization from ethanol.

General procedure for the synthesis of 1-phenyl-3-(4-(thiophen-2-yl)thiazol-2-yl)urea derivatives (TTU3, TTU5- TTU7, TTU9- TTU11, TTU13, TTU16)

4-(Thiophen-2-yl)thiazol-2-amine (**IV)** was added to equimolar amount of corresponding phenyl/naphthyl isocyanate (**V**) solution in 5-10 mL toluene. At 80 ° C, the mixture was mixed until complete and then chilled to room temperature. The precipitate was separated using filtration and washed with benzene. To obtain the urea derivatives, the resultant residue was purified by crystallization from ethanol.

1-(4-Bromophenyl)-3-(4-(thiophen-2-yl)thiazol-2-yl)urea (TTU1)

Pale brown solid. Yield: 45%. Mp: 192-194 °C. ^{1}H NMR (400 MHz, DMSO-d_6) δ 10.96 (s, 1H), 8.97 (s, 1H), 7.60 – 7.42 (m, 6H), 7.39 (s, 1H), 7.13 – 7.06 (m, 1H). ^{13}C NMR (100 MHz, DMSO) δ 160.95, 138.41, 138.35, 131.94, 131.71, 128.76, 128.59, 126.22, 125.62, 124.45, 106.20 (one carbon signal was overlapped). HRMS (EI): $[M+H]^+$, found 379,95499. $C_{14}H_{11}BrN_3OS_2$ requires 379,95269.

1-(4-Chlorophenyl)-3-(4-(thiophen-2-yl)thiazol-2-yl)urea (TTU2)

White-cream solid. Yield: 14%. Mp: 228-230 °C. ^{1}H NMR (400 MHz, DMSO-d_6) δ 10.94 (s, 1H), 9.01 (s, 1H), 7.57 – 7.45 (m, 4H), 7.41 – 7.30 (m, 3H), 7.13 – 7.06 (m, 1H). ^{13}C NMR (100 MHz, DMSO) δ 159.47, 151.88, 144.05, 138.87, 137.91, 129.23, 128.45, 126.91, 125.81, 124.03, 120.76, 106.13. HRMS (EI): $[M+H]^+$, found 336,00315. $C_{14}H_{11}ClN_3OS_2$ requires 336,00321.

1-(3-Fluorophenyl)-3-(4-(thiophen-2-yl)thiazol-2-yl)urea (TTU3)

White-cream solid. Yield: 77%. Mp: 192-194 °C. ^{1}H NMR (400 MHz, DMSO-d_6) δ 11.13 (s, 1H), 9.08 (s, 1H), 7.57 – 7.42 (m, 3H), 7.39 – 7.25 (m,2H), 7.19 – 7.13 (m, 1H), 7.12 – 7.04 (m,1H), 6.82 (t, J = 7.4 Hz, 1H). ^{13}C NMR (100 MHz, DMSO) δ 162.78 (d, J = 241.2 Hz), 152.91, 143.89, 141.32, 141.16, 139.09, 130.83 (d, J = 9.7 Hz), 128.39, 125.67, 123.88, 114.78, 109.26 (d, J = 20.7 Hz)., 105.80, 105.55. HRMS (EI): $[M+H]^+$, found 320,03221. $C_{14}H_{11}FN_3OS_2$ requires 320,03276.

1-(4-Fluorophenyl)-3-(4-(thiophen-2-yl)thiazol-2-yl)urea (TTU4)

Brown solid. Yield: 50%. Mp: 206-208 °C. ^{1}H NMR (400 MHz, DMSO-d_6) δ 10.89 (s, 1H), 8.85 (s, 1H), 7.56 – 7.45 (m, 3H), 7.37 (d, J = 3.1 Hz, 2H), 7.16 (t, J = 9.2 Hz, 2H), 7.13 – 7.06 (m, 1H). ^{13}C NMR (100 MHz, DMSO) δ 159.62, 158.35 (d, J = 239.4 Hz), 152.03, 144.00, 138.89, 135.19, 128.48, 125.81, 124.01, 121.16 (d, J = 7.8 Hz), 115.94 (d, J = 22.4 Hz), 106.05. HRMS (EI): $[M+H]^+$, found 320,03287. $C_{14}H_{11}FN_3OS_2$ requires 320,03276.

1-(3-Cyanophenyl)-3-(4-(thiophen-2-yl)thiazol-2-yl)urea (TTU5)

Yellow solid. Yield: 82%. Mp: 192-194 °C. ^{1}H NMR (400 MHz, DMSO-d_6) δ 11.14 (s, 1H), 9.15 (s, 1H), 7.98 (s, 1H), 7.73 (d, J = 7.6 Hz, 1H), 7.60 – 7.44 (m, 4H), 7.39 (s, 1H), 7.15 – 7.04 (m, 1H).^{13}C NMR (100 MHz, DMSO) δ 159.95, 152.26, 144.04, 139.97, 138.86, 130.74, 128.47, 126.72, 125.84, 124.05, 123.93, 121.84, 119.14, 112.13, 106.23. HRMS (EI): $[M-H]^+$, found 325,02233. $C_{15}H_9N_4OS_2$ requires 325,02178.

1-(4-Cyanophenyl)-3-(4-(thiophen-2-yl)thiazol-2-yl)urea (TTU6)

Yellow solid. Yield: 87%. Mp: 199-201 °C. ^{1}H NMR (400 MHz, DMSO-d_6) δ 11.20 (s, 1H), 9.37 (s, 1H), 7.75 (d, J = 8.6 Hz,2H), 7.67 (d, J = 8.7 Hz, 2H), 7.54 – 7.45 (m, 2H), 7.37 (s, 1H), 7.12 – 7.06 (m, 1H). ^{13}C NMR (100 MHz, DMSO) δ 159.17, 151.72, 144.13, 143.39, 142.58, 138.76, 133.86, 128.51, 125.92, 124.14, 119.54, 119.11, 106.42, 104.86. HRMS (EI): $[M-H]^+$, found 325,02233. $C_{15}H_9N_4OS_2$ requires 325,02178.

1-(4-(Thiophen-2-yl)thiazol-2-yl)-3-(4-(trifluoromethoxy)phenyl)urea (TTU7)

White-cream solid. Yield: 72%. Mp: 206-207 °C. ^{1}H NMR (400 MHz, DMSO-d_6) δ 11.02 (s, 1H), 9.02 (s, 1H), 7.60 (d, J = 9.0 Hz, 2H), 7.47 (d, J = 5.0 Hz, 2H), 7.40 – 7.22 (m, 3H), 7.20 – 6.98 (m, 1H). ^{13}C NMR (100 MHz, DMSO) δ 160.82, 153.19, 143.88, 143.46, 139.17, 138.69, 128.37, 125.63, 123.83, 122.15, 121.94, 120.29, 105.73. HRMS (EI): $[M+H]^+$, found 386,02393. $C_{15}H_{11}F_3N_3O_2S_2$ requires 386,02448.

1-(4-Nitrophenyl)-3-(4-(thiophen-2-yl)thiazol-2-yl)urea (TTU8)

Yellow solid. Yield: 45%. Mp: 275-277 °C. ^{1}H NMR (400 MHz, DMSO-d_6) δ 11.15 (s, 1H), 9.50 (s, 1H), 8.22 (d, J = 9.2 Hz, 2H), 7.73 (d, J = 9.2 Hz, 2H), 7.54 – 7.47 (m, 2H), 7.44 (s, 1H), 7.13 – 7.06 (m, 1H). ^{13}C NMR (101 MHz, DMSO) δ 159.10, 151.69, 145.46, 144.19, 142.31, 138.76, 128.48, 125.93, 125.59, 124.18, 118.69, 106.54. HRMS (EI): $[M+H]^+$, found 347,03116. $C_{14}H_{11}N_4O_3S_2$ requires 347,02726.

1-(4-(Thiophen-2-yl)thiazol-2-yl)-3-(m-tolyl)urea (TTU9)

White-cream solid. Yield: 79%. Mp: 200-202 °C. ^{1}H NMR (400 MHz, DMSO-d_6) δ 10.89 (s, 1H), 8.74 (s, 1H), 7.53 – 7.43 (m, 2H), 7.35 (s, 1H), 7.31 (s, 1H), 7.25 (d, J = 7.9 Hz, 1H), 7.23 – 7.14 (m, 1H), 7.13 – 7.04 (m, 1H), 6.85 (d, J = 7.1 Hz, 1H), 2.29 (s, 3H). ^{13}C NMR (100 MHz,

DMSO) δ 159.62, 151.87, 143.99, 138.92, 138.80, 138.69, 129.23, 128.45, 125.79, 124.05, 123.99, 119.58, 116.26, 105.96, 40.58, 40.37, 21.59. HRMS (EI): $[M+H]^+$, found 316,05943. $C_{15}H_{14}N_3OS_2$ requires 316,05783.

1-(4-(Thiophen-2-yl)thiazol-2-yl)-3-(p-tolyl)urea (TTU10)

Pale yellow solid. Yield: 57%. Mp: 175-177 °C. ^{1}H NMR (400 MHz, DMSO-d_6) δ 10.91 (s, 1H), 8.73 (s, 1H), 7.51 – 7.44 (m, 2H), 7.42 – 7.29 (m,3H), 7.23 – 7.01 (m, 3H), 2.25 (s, 3H). ^{13}C NMR (100 MHz, DMSO) δ 159.73, 151.93, 143.94, 138.88, 136.24, 132.34, 129.78, 128.49, 125.77, 123.98, 119.24, 105.92, 20.81. HRMS (EI): $[M+H]^+$, found 316,05943. $C_{15}H_{14}N_3OS_2$ requires 316,05783.

1-(4-(Tert-butyl)phenyl)-3-(4-(thiophen-2-yl)thiazol-2-yl)urea (TTU11)

Yellow solid. Yield: 29%. Mp: 196-198 °C. ^{1}H NMR (400 MHz, DMSO-d_6) δ 10.72 (s, 1H), 8.72 (s, 1H), 7.49 – 7.41 (m, 2H), 7.42 – 7.35 (m, 2H), 7.32 – 7.22 (m, 3H), 7.12 – 7.03 (m, 1H), 1.26 (s, 9H). ^{13}C NMR (100 MHz, DMSO) δ 160.87, 152.84, 145.31, 143.85, 139.20, 136.66, 128.37, 125.89, 125.60, 123.80, 118.83, 105.55, 34.39, 31.68. HRMS (EI): $[M+H]^+$, found 358,10423. $C_{18}H_{20}N_3OS_2$ requires 358,10478.

1-(4-Methoxyphenyl)-3-(4-(thiophen-2-yl)thiazol-2-yl)urea (TTU12)

White solid. Yield: 51%. Mp: 187-189 °C. ^{1}H NMR (400 MHz, DMSO-d_6) δ 10.82 (s, 1H), 8.63 (s, 1H), 7.50 – 7.43 (m, 2H), 7.41 – 7.27 (m, 3H), 7.08 (dd, J = 5.0, 3.7 Hz, 1H), 6.89 (d, J = 8.8 Hz, 2H), 3.72 (s, 3H). ^{13}C NMR (101 MHz, DMSO) δ 158.72, 155.48, 143.89, 139.08, 131.99, 128.78, 128.43, 125.68, 123.86, 120.97, 114.50, 105.69, 55.64. HRMS (EI): $[M+H]^+$, found 332,05219. $C_{15}H_{14}N_3O_2S_2$ requires 332,05274.

1-(4-Chloro-3-(trifluoromethyl)phenyl)-3-(4-(thiophen-2-yl)thiazol-2-yl)urea (TTU13)

White-cream solid. Yield: 90%. Mp: 205-207 °C. ^{1}H NMR (400 MHz, DMSO-d_6) δ 11.17 (s, 1H), 9.40 (s, 1H), 8.08 (d, J = 2.4 Hz, 1H), 7.72 (dd, J = 8.7, 2.3 Hz, 1H), 7.64 (d, J = 8.8 Hz, 1H), 7.51 – 7.42 (m, 2H), 7.39 (s, 1H), 7.23 – 6.99 (m, 1H).^{13}C NMR (100 MHz, DMSO) δ 160.76, 152.97, 143.92, 139.01, 138.93, 132.42, 128.75, 128.36, 125.71, 124.54, 123.99, 123.96, 123.47, 117.73, 106.07. HRMS (EI): $[M+H]^+$, found 403,99614. $C_{15}H_{10}ClF_3N_3OS_2$ requires 403,99059.

1-(3,4-Dimethoxyphenyl)-3-(4-(thiophen-2-yl)thiazol-2-yl)urea (TTU14)

White-cream solid. Yield: 25%. Mp: 185-187 °C. ^{1}H NMR (400 MHz, DMSO-d_6) δ 10.97 (s, 1H), 8.73 (s, 1H), 7.47 (t, J = 4.2 Hz, 2H), 7.41 – 7.30 (m, 1H), 7.15 (d, J = 2.0 Hz, 1H), 7.08 (dd, J = 5.1, 3.6 Hz, 1H), 6.92 (dd, J = 8.5, 2.3 Hz, 1H), 6.88 (d, J = 8.4 Hz, 1H), 3.73 (s, 3H), 3.71 (s, 3H). ^{13}C NMR (100 MHz, DMSO) δ 160.21, 152.30, 149.29, 145.15, 143.91, 139.03, 132.49, 128.41, 125.69, 123.91, 112.85, 111.26, 105.76, 104.74, 56.29, 55.92. HRMS (EI): $[M+H]^+$, found 362,06276. $C_{16}H_{16}N_3O_3S_2$ requires 362,06331.

1-(3,4,5-Trimethoxyphenyl)-3-(4-(thiophen-2-yl)thiazol-2-yl)urea (TTU15)

White solid. Yield: 51%. Mp: 229-231 °C. ^{1}H NMR (400 MHz, DMSO-d_6) δ 10.87 (s, 1H), 8.75 (s, 1H), 7.56 – 7.45 (m, 2H), 7.37 (s, 1H), 7.17 – 7.04 (m, 1H), 6.81 (s, 2H), 3.77 (s, 6H), 3.62 (s, 3H). ^{13}C NMR (100 MHz, DMSO) δ 159.63, 153.40, 151.88, 144.01, 138.91, 134.93, 133.75, 128.44, 125.78, 124.02, 105.99, 97.15, 60.58, 56.29. HRMS (EI): $[M+H]^+$, found 392,07332. $C_{17}H_{18}N_3O_4S_2$ requires 392,07387.

1-(Naphthalen-2-yl)-3-(4-(thiophen-2-yl)thiazol-2-yl)urea (TTU16)

Yellow solid. Yield: 62%. Mp: 176-179 °C. ^{1}H NMR (400 MHz, DMSO-d_6) δ 11.20 (s, 1H), 9.04 (s, 1H), 8.11 (d, J = 5.9 Hz, 1H), 8.05 (d, J = 7.4 Hz, 1H), 7.97 (d, J = 7.6 Hz, 1H), 7.73 (d, J = 5.9 Hz, 1H), 7.65 – 7.44 (m, 4H), 7.43 – 7.34 (m, 2H), 7.17 – 7.03 (m, 1H). ^{13}C NMR (100 MHz, DMSO) δ 159.69, 152.32, 144.06, 138.92, 134.12, 133.54, 128.98, 128.77, 128.50, 126.65, 126.58, 126.29, 125.85, 124.39, 124.02, 121.43, 118.15, 106.01. HRMS (EI): $[M+H]^+$, found 352,05728. $C_{18}H_{14}N_3OS_2$ requires 352,05783.

4.2. Biological evaluation

4.2.1. MABA Protocol

Mycobacterium tuberculosis H37Rv and isoniazid-resistant *Mtb* clinical isolates were inoculated from a freezer stock into 7H9+OADC and grown to mid-log phase. Logarithmically growing *Mtb* was then inoculated into Sauton's medium in 96 well plates with wells containing increasing concentrations of test compounds at an ODλ600 of 0.0008, corresponding to approximately 4x105 CFU/mL in 200 µL per well. Plates were incubated at 37˚C for 1 week,

at which point 32.5 µL of a resazurin-tween mixture (8:5 ratio of 0.6mM Resazurin in 1X PBS to 20% Tween 80) was added and the plate was incubated at 37˚C overnight. Production of fluorescent resorufin was measured by removing samples from the plate, mixing with formalin to kill the *Mtb*, and measuring the fluorescence on a VictorNivo plate reader using filters 530/30nm for excitation and 580/20 nm for emission. For each assay, media alone served as a negative control and untreated *Mtb* was included as a positive control. The % inhibition was calculated as the ((positive control - negative control) - (fluorescence of the sample - negative control))/(positive control - negative control) x 100%. GraphPad Prism 8 was used to calculate the MIC50 values [30,31].

4.2.2. Cytotoxicity determination (MTT assay protocol)

To determine the toxicity of the compounds against normal host cells (macrophages), we used the MTT (3-(4,5-dimethylthiazol-2-yl)-2,5-diphenyltetrazolium bromide) assay. Cell toxicity was tested using an inhibition assay with HEK cell lines. Various concentrations of compounds were added to sterile 96 well microtiter plate having 5×103 cells and incubated for 48 h at 37 °C. After the incubation period, 10 µl of 3-(4,5-dimethylthiazol-2-yl)-2,5-di-phenyltetrazolium bromide (MTT reagent) (5 mg/mL) was added and then incubated for 3 h. Next, media was removed and 100 µl of DMSO was added to each well. DMSO dissolves the formazan crystals formed in wells. The absorbance was measured at 560 nm using Perkin Elmer Victor X3 microplate reader against the blank. The assay was performed in triplicates for each concentration. The cytotoxicity is represented as % inhibition at each concentration. The data were normalized with the lowest and highest values and subjected to non-linear regression analysis to obtain log (concentration) vs normalized expression (variable slope) using Graphpad Prism. The IC_{50} (inhibition of cell growth) concentrations were further obtained using Graphpad Prism.

4.2.3. InhA inhibition assay

InhA expression and purification

The plasmid pET15b/InhA was ordered from GeneScript. InhA DNA sequence was found in UniProt and codon optimization was performed using the algorithm furnished by Genescript. Production and purification of the InhA-His_6 protein from strain of *E. coli* BL21(DE3) transformed with the pET15b/InhA plasmid were performed as described.[21] The His_6 tagged protein was concentrated to 5 µM in PIPES buffer and was used for the enzymatic assays without further optimization.

InhA activity inhibition

NADH was obtained from Alfa Aesar. Stock solutions of all compounds were prepared in DMSO. *trans*-2-Dodecenoyl-coenzyme A (DDCoA) was synthesized from trans-2-dodecenoic acid and commercialy available coenzyme A trilithium salt (Sigma-Aldrich) using the mixed anhydrid method [32]. Kinetic assays were performed at 25°C in 30 mM PIPES and 150 mM NaCl at pH 6.8, containing 250 µM cofactor (NADH), 50 µM substrate (DDCoA) and the tested compound (at 50 µM for all compounds; at 10 µM and 50 µM for TTU1) [32]. The final concentration of DMSO is 5% (v/v). Reactions were initiated by addition of InhA (100 nM final) and NADH oxidation was followed at 340 nm. The inhibitory activity of each derivative was expressed as the percentage inhibition of InhA activity (initial velocity of the reaction) with respect to the control reaction without inhibitor. All activity assays were performed in duplicate or triplicate if inhibition is observed.

4.3. Molecular docking

The chemical structure of **TTU1** with the best InhA inhibition value was drawn and energy minimized using the MMFF94 force field in LigandScout [33]. The crystal structure of InhA enzyme with a urea-based ligand (1-cyclohexyl-3-(pyridin-3-ylmethyl)urea) under PDB Code:5OIL [34] was downloaded from Protein Data Bank. **TTU1** was docked into the binding pocket of InhA using AutoDock 4.2 [35], implemented in LigandScout with default parameters. The obtained docking poses were visually analyzed in LigandScout. Finally, the figures were prepared using Discovery Studio [36] and LigandScout.

Conflict of Interest

The authors declared no potential conflicts of interest.

Acknowledgments

MGG is grateful to Prof. Dr. Gerhard Wolber, Freie Universität Berlin, for providing the license for LigandScout 4.2.

References

[1] S. Tiberi, M. Muñoz-Torrico, R. Duarte, M. Dalcolmo, L. D'Ambrosio, G.-B. Migliori, New drugs and perspectives for new anti-tuberculosis regimens, Pulmonology. 24 (2018) 86–98. doi:10.1016/J.RPPNEN.2017.10.009.

[2] WHO, Global Tuberculosis Report 2020, (n.d.). https://www.who.int/teams/global-tuberculosis-programme/tb-reports/global-tuberculosis-report-2020.

[3] D.T. Hoagland, J. Liu, R.B. Lee, R.E. Lee, New agents for the treatment of drug-resistant Mycobacterium tuberculosis, Adv. Drug Deliv. Rev. 102 (2016) 55–72. doi:10.1016/J.ADDR.2016.04.026.

[4] R. Singh, S.P. Dwivedi, U.S. Gaharwar, R. Meena, P. Rajamani, T. Prasad, Recent updates on drug resistance in *Mycobacterium tuberculosis*, J. Appl. Microbiol. 128 (2020) 1547–1567. doi:10.1111/jam.14478.

[5] M. T. Chhabria, S. Patel, P. Modi, P. S. Brahmkshatriya, Thiazole: A Review on Chemistry, Synthesis and Therapeutic Importance of its Derivatives, Curr. Top. Med. Chem. 16 (2016) 2841–2862. doi:10.2174/1568026616666160506130731.

[6] A. Ayati, S. Emami, S. Moghimi, A. Foroumadi, Thiazole in the targeted anticancer drug discovery, Future Med. Chem. 11 (2019) 1929–1952. doi:10.4155/fmc-2018-0416.

[7] C.B. Mishra, S. Kumari, M. Tiwari, Thiazole: A promising heterocycle for the development of potent CNS active agents, Eur. J. Med. Chem. 92 (2015) 1–34. doi:10.1016/j.ejmech.2014.12.031.

[8] S.J. Kashyap, V.K. Garg, P.K. Sharma, N. Kumar, R. Dudhe, J.K. Gupta, Thiazoles: Having diverse biological activities, Med. Chem. Res. 21 (2012) 2123–2132. doi:10.1007/s00044-011-9685-2.

[9] S. Pola, Significance of Thiazole-based Heterocycles for Bioactive Systems, in: Scope Sel. Heterocycles from Org. Pharm. Perspect., InTech, 2016. doi:10.5772/62077.

[10] C.B. Scarim, F.R. Pavan, Thiazole, triazole, thio- and semicarbazone derivatives - Promising moieties for drug development for the treatment of tuberculosis, Eur. J. Med. Chem. Reports. 1 (2021) 100002. doi:10.1016/j.ejmcr.2021.100002.

[11] R. Mishra, I. Tomar, S. Singhal, K.K. Jha, Synthesis, properties and biological activity of thiophene: A review, Der Pharma Chem. 3 (2011) 38–54.

[12] R. Liu, X. Lyu, S.M. Batt, M.-H. Hsu, M.B. Harbut, C. Vilchèze, B. Cheng, K. Ajayi, B. Yang, Y. Yang, H. Guo, C. Lin, F. Gan, C. Wang, S.G. Franzblau, W.R. Jacobs,

G.S. Besra, E.F. Johnson, M. Petrassi, A.K. Chatterjee, K. Fütterer, F. Wang, Determinants of the Inhibition of DprE1 and CYP2C9 by Antitubercular Thiophenes, Angew. Chemie. 129 (2017) 13191–13195. doi:10.1002/ange.201707324.

[13] R. Mishra, N. Sachan, N. Kumar, I. Mishra, P. Chand, Thiophene Scaffold as Prospective Antimicrobial Agent: A Review, J. Heterocycl. Chem. 55 (2018) 2019–2034. doi:10.1002/jhet.3249.

[14] A.K. Ghosh, M. Brindisi, Urea Derivatives in Modern Drug Discovery and Medicinal Chemistry, J. Med. Chem. (2019). doi:10.1021/acs.jmedchem.9b01541.

[15] J.R. Brown, E.J. North, J.G. Hurdle, C. Morisseau, J.S. Scarborough, D. Sun, J. Korduláková, M.S. Scherman, V. Jones, A. Grzegorzewicz, R.M. Crew, M. Jackson, M.R. McNeil, R.E. Lee, The structure-activity relationship of urea derivatives as anti-tuberculosis agents, Bioorganic Med. Chem. 19 (2011) 5585–5595. doi:10.1016/j.bmc.2011.07.034.

[16] R. Ronchetti, G. Moroni, A. Carotti, A. Gioiello, E. Camaioni, Recent advances in urea- and thiourea-containing compounds: focus on innovative approaches in medicinal chemistry and organic synthesis, RSC Med. Chem. (2021). doi:10.1039/d1md00058f.

[17] M.S. Prasad, R.P. Bhole, P.B. Khedekar, R. V. Chikhale, Mycobacterium enoyl acyl carrier protein reductase (InhA): A key target for antitubercular drug discovery, Bioorg. Chem. 115 (2021) 105242. doi:10.1016/j.bioorg.2021.105242.

[18] N. Tahiri, P. Fodran, D. Jayaraman, J. Buter, M.D. Witte, T.A. Ocampo, D.B. Moody, I. Van Rhijn, A.J. Minnaard, Total Synthesis of a Mycolic Acid from Mycobacterium tuberculosis , Angew. Chemie. 132 (2020) 7625–7630. doi:10.1002/ange.202000523.

[19] H. Marrakchi, G. Lanéelle, A. Quémard, InhA, a target of the antituberculous drug isoniazid, is involved in a mycobacterial fatty acid elongation system, FAS-II, Microbiology. 146 (2000) 289–296. doi:10.1099/00221287-146-2-289.

[20] A. Campaniço, R. Moreira, F. Lopes, Drug discovery in tuberculosis. New drug targets and antimycobacterial agents, Eur. J. Med. Chem. 150 (2018) 525–545. doi:10.1016/J.EJMECH.2018.03.020.

[21] A. Chollet, L. Mourey, C. Lherbet, A. Delbot, S. Julien, M. Baltas, J. Bernadou, G. Pratviel, L. Maveyraud, V. Bernardes-Génisson, Crystal structure of the enoyl-ACP reductase of Mycobacterium tuberculosis (InhA) in the apo-form and in complex with the active metabolite of isoniazid pre-formed by a biomimetic approach, J. Struct. Biol. 190 (2015) 328–337. doi:10.1016/j.jsb.2015.04.008.

[22] J.N. Torres, L. V. Paul, T.C. Rodwell, T.C. Victor, A.M. Amallraja, A. Elghraoui, A.P.

Goodmanson, S.M. Ramirez-Busby, A. Chawla, V. Zadorozhny, E.M. Streicher, F.A. Sirgel, D. Catanzaro, C. Rodrigues, M.T. Gler, V. Crudu, A. Catanzaro, F. Valafar, Novel katG mutations causing isoniazid resistance in clinical M. Tuberculosis isolates, Emerg. Microbes Infect. 4 (2015) e42. doi:10.1038/emi.2015.42.

[23] A. Chollet, L. Maveyraud, C. Lherbet, V. Bernardes-Génisson, An overview on crystal structures of InhA protein: Apo-form, in complex with its natural ligands and inhibitors, Eur. J. Med. Chem. 146 (2018) 318–343. doi:10.1016/J.EJMECH.2018.01.047.

[24] V.R. Bollela, E.I. Namburete, C.S. Feliciano, D. Macheque, L.H. Harrison, J.A. Caminero, Detection of katG and inhA mutations to guide isoniazid and ethionamide use for drug-resistant tuberculosis, Int. J. Tuberc. Lung Dis. 20 (2016) 1099–1104. doi:10.5588/ijtld.15.0864.

[25] G. Gudipudi, S.R. Sagurthi, S. Perugu, G. Achaiah, G.L.D. Krupadanam, Rational design and synthesis of novel 2-(substituted-2H-chromen-3-yl)-5-aryl-1H-imidazole derivatives as an anti-angiogenesis and anti-cancer agent, RSC Adv. 4 (2014) 56489–56501. doi:10.1039/c4ra09945a.

[26] A.M. Farag, H.M. Hassaneen, I.M. Abbas, A.S. Shawali, M.S. Algharib, Synthesis and reactions of some 2-thienyl- and 2-thenoyl-derivatives of thiazole and thiadiazoline and their selenium analogs, Phosphorous Sulfur Relat. Elem. 40 (1988) 243–249. doi:10.1080/03086648808072921.

[27] T. Meşeli, Ş.D. Doğan, M.G. Gündüz, Z. Kökbudak, S. Skaro Bogojevic, T. Noonan, S. Vojnovic, G. Wolber, J. Nikodinovic-Runic, Design, synthesis, antibacterial activity evaluation and molecular modeling studies of new sulfonamides containing a sulfathiazole moiety, New J. Chem. 45 (2021) 8166–8177. doi:10.1039/d1nj00150g.

[28] Ş.D. Doğan, Copper-catalyzed NH/SH functionalization: A strategy for the synthesis of benzothiadiazine derivatives, Tetrahedron. 73 (2017) 2217–2224. doi:10.1016/J.TET.2017.02.063.

[29] M.G. Gündüz, S.B. Uğur, F. Güney, C. Özkul, V.S. Krishna, S. Kaya, D. Sriram, Ş.D. Doğan, 1,3-Disubstituted urea derivatives: Synthesis, antimicrobial activity evaluation and in silico studies, Bioorg. Chem. 102 (2020) 104104. doi:10.1016/j.bioorg.2020.104104.

[30] V.S. Krishna, S. Zheng, E.M. Rekha, R. Nallangi, D. V. Sai Prasad, S.E. George, L.W. Guddat, D. Sriram, Design and development of ((4-methoxyphenyl)carbamoyl) (5-(5-nitrothiophen-2-yl)-1,3,4-thiadiazol-2-yl)amide analogues as Mycobacterium

tuberculosis ketol-acid reductoisomerase inhibitors, Eur. J. Med. Chem. 193 (2020) 112178. doi:10.1016/j.ejmech.2020.112178.

[31] K. Flentie, G.A. Harrison, H. Tükenmez, J. Livny, J.A.D. Good, S. Sarkar, D.X. Zhu, R.L. Kinsella, L.A. Weiss, S.D. Solomon, M.E. Schene, M.R. Hansen, A.G. Cairns, M. Kulén, T. Wixe, A.E.G. Lindgren, E. Chorell, C. Bengtsson, K.S. Krishnan, S.J. Hultgren, C. Larsson, F. Almqvist, C.L. Stallings, Chemical disarming of isoniazid resistance in Mycobacterium tuberculosis, Proc. Natl. Acad. Sci. U. S. A. 116 (2019) 10510–10517. doi:10.1073/pnas.1818009116.

[32] A. Chollet, G. Mori, C. Menendez, F. Rodriguez, I. Fabing, M.R. Pasca, J. Madacki, J. Korduláková, P. Constant, A. Quémard, V. Bernardes-Génisson, C. Lherbet, M. Baltas, Design, synthesis and evaluation of new GEQ derivatives as inhibitors of InhA enzyme and Mycobacterium tuberculosis growth, Eur. J. Med. Chem. 101 (2015) 218–235. doi:10.1016/j.ejmech.2015.06.035.

[33] G. Wolber, T. Langer, LigandScout: 3-D pharmacophores derived from protein-bound ligands and their use as virtual screening filters, J. Chem. Inf. Model. 45 (2005) 160–169. doi:10.1021/ci049885e.

[34] F. Prati, F. Zuccotto, D. Fletcher, M.A. Convery, R. Fernandez-Menendez, R. Bates, L. Encinas, J. Zeng, C. Chung, P. De Dios Anton, A. Mendoza-Losana, C. Mackenzie, S.R. Green, M. Huggett, D. Barros, P.G. Wyatt, P.C. Ray, Screening of a Novel Fragment Library with Functional Complexity against *Mycobacterium tuberculosis* InhA, ChemMedChem. 13 (2018) 672–677. doi:10.1002/cmdc.201700774.

[35] G.M. Morris, R. Huey, W. Lindstrom, M.F. Sanner, R.K. Belew, D.S. Goodsell, A.J. Olson, AutoDock4 and AutoDockTools4: Automated docking with selective receptor flexibility, J. Comput. Chem. 30 (2009) 2785–2791. doi:10.1002/jcc.21256.

[36] Dassault Systemes Biovia, Discovery Studio Visualizer, Version 4.1.34, (2016).